CeOx/Co-NC catalysts under various conditions for Electrochemical Nitrate Reduction Reaction to Ammonia

Anas Alsaadi, Guanjie He, Zeyu Geng

anas.alsaadi@kaust.edu.sa, g.he@ucl.ac.uk, zeyu.geng.24@ucl.ac.uk

Abstract

The electrochemical nitrate reduction reaction (NO_3^-RR) offers a route to convert nitrate pollutants into ammonia (NH_3) under ambient conditions. In this work, an unsupported MOF-derived Co-NC electrocatalyst – cobalt single-site/nanoparticle centers supported on a nitrogen-doped carbon nanosphere network – was evaluated for NO_3^-RR to NH_3 and benchmarked against a 3D porous Co-NC@Fe foam architecture. The catalysts were tested across applied potentials of −0.4 to −0.8 V vs. RHE in Na_2SO_4 supporting electrolyte. By systematically scaling the reactant concentration from 0.1 M to 1.0 M KNO_3, mass transport and diffusion limitations were overcome. The optimized unsupported Co-NC powder achieved a commercial-scale NH_3 yield rate of ~1.9 mmol h^{-1} cm^{-2} at −0.8 V/1.0 M KNO_3 while maintaining a high Faradaic efficiency of >90%. Conversely, the 3D Co-NC@Fe foam suffered a severe performance collapse due to parasitic hydrogen evolution on the iron support and physical suffocation from gas bubbles trapped in its macroscopic voids. These results demonstrate that open, non-trapping nanosphere morphologies are superior for high-throughput ammonia electrosynthesis.

Date: August 24, 2026

Contents

1 Introduction **2**

1.1 Problem statement . . . 2

1.2 This work . . . 2

2 Related Work **3**

2.1 Dual-site / tandem catalysis for hydrogen supply . . . 3

2.2 Lattice/electronic modulation by an oxide component . . . 3

3 Methodology **4**

3.1 Catalyst Preparation . . . 4

3.2 Electrochemical Experimental Setup . . . 4

3.3 Product Quantification and Performance Metrics . . . 4

4 Results **5**

4.1 Concentration Optimization . . . 5

4.2 The 3D Support Trap and Morphological Analysis . . . 5

5 Discussion **6**

6 Limitations and Future Work **6**

7 Conclusion and Future Outlook **7**

References **8**

1 Introduction

Ammonia (NH_3) is one of the most heavily produced chemicals in the world, underpinning nitrogen fertilizer for global food security and increasingly discussed as a carbon-free hydrogen carrier and marine fuel [1]. Nearly all of today's NH_3 is made by the Haber–Bosch process, which reacts N_2 with H_2 at high temperature (~400–500°C) and pressure (>100 atm). This process consumes 1–2% of global energy supply and is responsible for a comparable share of global CO_2 emissions, since the H_2 feedstock is overwhelmingly produced from fossil fuels via steam methane reforming [1, 2].

At the same time, nitrate (NO_3^-) is one of the most widespread water contaminants, arising from agricultural runoff (over-application of fertilizer), industrial wastewater, and livestock waste. Excess nitrate in groundwater and surface water is a direct threat to human health and aquatic ecosystems [2]. The electrochemical nitrate reduction reaction (NO_3^-RR) converts this pollutant directly into NH_3 under ambient temperature and pressure, powered by electricity that can be sourced from renewables. Compared to N_2 reduction, NO_3^- is a far more attractive nitrogen source: the N=O bond in nitrate (~204 kJ mol^{-1}) is much weaker than the N≡N triple bond in N_2 (941 kJ mol^{-1}), and NO_3^- is highly soluble in water, so NO_3^-RR simultaneously achieves water remediation and ammonia synthesis [2, 3].

1.1 Problem statement

NO_3^-RR to NH_3 is a demanding nine-proton, eight-electron transfer reaction:

$$NO_3^- + 6\,H_2O + 8\,e^- \rightarrow NH_3 + 9\,OH^- \qquad (E^0 = 0.69\ \text{V vs. RHE},\ \text{pH 14}) \tag{1}$$

The reaction proceeds through a cascade of deoxygenation and hydrogenation steps ($NO_3^- \rightarrow NO_2^- \rightarrow NO \rightarrow \cdots \rightarrow NH_3$), and the partially reduced nitrite (NO_2^-) intermediate is itself a regulated pollutant, so a good catalyst must not only be active but also highly *selective* toward the eight-electron NH_3 product rather than stalling at NO_2^- or over-reducing toward N_2/N_2O. In addition, the competing hydrogen evolution reaction (HER) consumes protons and electrons without producing NH_3, and becomes more severe at the very negative potentials often needed to drive NO_3^-RR at useful rates. A recurring design principle in recent literature is to pair a site that binds and activates NO_3^-/NO_x intermediates with a second site or feature that supplies active hydrogen (*H) from water dissociation, so that hydrogenation of the nitrogen intermediates is not rate-limiting [4–7].

1.2 This work

We evaluate a MOF-derived Co-NC catalyst (cobalt single-sites/nanoparticles on nitrogen-doped carbon nanospheres) for NO_3^-RR to NH_3. To address mass transport limitations, we systematically scale the reactant concentration from 0.1 M to 1.0 M KNO_3. Furthermore, we evaluate the impact of the catalyst architecture by benchmarking the unsupported Co-NC powder against a 3D porous Co-NC@Fe foam. We demonstrate how substrate choices can lead to unintended parasitic reactions and gas trapping. The key assumptions and scope of this study are:

- All experiments are conducted in an H-type (divided) cell with a fixed electrolyte composition class (Na_2SO_4 + KNO_3).
- Only NH_3 and NO_2^- are quantified as products.
- Faradaic efficiency (FE) and yield rate are derived from the recorded electrochemical measurements.

2 Related Work

Table 1 summarizes recent high-performing NO_3^-RR electrocatalysts and the design strategy each uses. Two themes recur across this literature and directly motivate the Co-NC design studied here.

Table 1 Representative NO_3^-RR electrocatalysts and their design strategy for coupling nitrate activation with active-hydrogen supply.

Catalyst	Strategy	Max FE_{NH_3}	Ref.
$Ru_{15}Co_{85}$ HNDs	Three-step relay mechanism	97%	[1]
OD-Cu nanosheets	Lattice oxygen + tensile strain	99.7%	[5]
Fe/Cu-HNG	Heteroatomic diatomic sites	92.5%	[8]
Cu^s/La^n-m	Metal cluster as proton donor	97.7%	[4]
Ni-BDC@Co-HHTP	MOF-on-MOF dual sites, built-in field	98.4%	[7]
Rh@Cu nanowires	H spillover from Rh to Cu	93%	[6]
Co-NC (this work)	**Oxide-modulated Co-N_x/C sites**	**~97%**	–

2.1 Dual-site / tandem catalysis for hydrogen supply

Because NO_3^-RR requires nine protons and eight electrons per NH_3 molecule, catalysts whose only active site is a metal that poorly dissociates water (e.g., bare Cu) tend to be rate-limited by hydrogen supply at low overpotential. Liu et al. addressed this by dispersing Rh clusters/single atoms on Cu nanowires (Rh@Cu): Rh supplies adsorbed *H via hydrogen spillover to *NO adsorbed on neighboring Cu sites, lowering the potential needed for hydrogenation and giving an NH_3 partial current density of 162 mA cm^{-2} and 93% FE at only −0.2 V vs. RHE [6]. Han et al. used a similar logic with a "three-step relay" on Ru_xCo_y alloys, in which Co first undergoes a spontaneous chemical redox with NO_3^- (forming $Co(OH)_2$ and NO_2^-), $Co(OH)_2$ is then electrochemically reduced back to Co, and Ru supplies active hydrogen for the NO_2^--to-NH_3 step – together lowering the onset potential to +0.4 V vs. RHE [1]. Zuo et al. took the same principle further by using La-based nanoparticles as a dedicated proton donor next to Cu single atoms (Cu^s/La^n): the La surface dissociates water and spills over *H to adjacent Cu sites, which bind and reduce NO_3^- via an "O-end" pathway, achieving 97.7% FE and 10.6 mol g_{metal}^{-1} h^{-1} [4]. Zou et al. similarly engineered a MOF-on-MOF heterostructure (Ni-BDC@Co-HHTP) where interfacial Ni–O–Co bonds create adjacent NO_3^--adsorbing (Ni) and water-dissociating (Co) sites, plus a built-in electric field from the two MOFs' different Fermi levels, reaching 98.4% FE [7].

2.2 Lattice/electronic modulation by an oxide component

A second strategy modifies the electronic structure of the active metal using an oxide or oxygen species rather than a second metal. Wu et al. showed that oxide-derived Cu nanosheets (OD-Cu) retain residual lattice oxygen and lattice tensile strain after electroreduction: the lattice oxygen withdraws electron density from surface Cu, weakening *NO_2 adsorption and relieving nitrite poisoning, while the tensile strain lowers the barrier for water dissociation to *H, together giving FE up to 99.7% [5]. Zhang et al. instead paired two different metals directly (Fe/Cu diatomic sites on N-doped graphene), showing that the heteroatomic Fe–Cu dimer weakens the N–O bond of adsorbed NO more than either homoatomic Fe–Fe or Cu–Cu dimer, while Fe supplies stronger NO_3^- adsorption than Cu [8].

Co-NC studied in this report follows the same conceptual family as these designs: Co-NC provides nitrogen-coordinated, carbon-supported cobalt sites for NO_3^- adsorption/activation (analogous to the metal–N_x sites in Fe/Cu-HNG or Ni-BDC), while the Co-NC component is expected to act similarly to the lattice oxygen in OD-Cu or the La clusters in Cu^s/La^n – modulating the Co electronic structure and/or assisting water dissociation to supply active hydrogen, suppressing NO_2^- accumulation relative to the Co-NC control. A gap in the reviewed literature is that most of the above studies report performance at a single, typically dilute nitrate concentration (10–100 mM); fewer systematically report how FE and yield rate evolve from 0.1 M to 1.0 M KNO_3 on the same catalyst, which is one of the axes explored in this report.

3 Methodology

3.1 Catalyst Preparation

The active materials were synthesized via a bottom-up metal-organic framework (MOF) self-assembly process. A precursor solution comprising cobalt salts (Co^{2+}) and organic ligands was stirred and aged to form a highly crystalline Co-MOF. This precursor underwent pyrolysis in an inert argon atmosphere. This thermal treatment carbonized the organic framework and anchored single cobalt atoms within a robust nitrogen-doped carbon matrix, yielding the unsupported Co-NC powder catalyst.

For the supported catalyst architecture, an identical precursor solution was utilized. However, in-situ growth was facilitated by immersing a 3D porous iron (Fe) foam into the solution prior to aging. The resulting Co-MOF@Fe foam was subsequently pyrolyzed under identical inert conditions to produce the Co-NC@Fe foam working electrode.

3.2 Electrochemical Experimental Setup

All electrochemical reduction experiments were performed in a standard three-electrode cell configuration. The synthesized Co-NC powder (drop-cast onto a conductive substrate) or the free-standing Co-NC@Fe foam served as the working electrode. A platinum (Pt) wire and an Ag/AgCl electrode were utilized as the counter and reference electrodes, respectively.

Constant potential electrolysis was executed across a targeted voltage window of −0.4 V to −0.8 V vs. RHE. Testing was conducted in a Na_2SO_4 supporting electrolyte spiked with systematically varying concentrations of KNO_3 (0.1 M, 0.5 M, and 1.0 M) to map the kinetic response and address mass transport limitations.

3.3 Product Quantification and Performance Metrics

After each controlled-potential electrolysis, the catholyte was sampled and analyzed by UV-Vis colorimetric assays (indophenol blue for NH_3 and Griess reagent for NO_2^-). The Faradaic efficiency (FE) for each product was computed based on the charge passed and the measured concentration, assuming 8 electrons for NH_3 and 2 electrons for NO_2^-.

4 Results

4.1 Concentration Optimization

The unsupported Co-NC catalyst demonstrated exceptional baseline selectivity in a 0.1 M KNO_3 electrolyte (Figure 1, left). It achieved a peak Faradaic Efficiency (FE) of ~96% at −0.5 V vs. RHE, effectively suppressing the NO_2^- intermediate.

To overcome mass transport and diffusion limitations, the reactant concentration was systematically scaled to 0.5 M (Figure 1, center) and 1.0 M KNO_3 (Figure 1, right). This optimization shattered the diffusion bottleneck, surging the absolute NH_3 yield to a commercial-scale maximum of ~1.9 mmol h^{-1} cm^{-2} at −0.8 V vs. RHE. Crucially, the Co-NC active sites strongly resisted parasitic hydrogen evolution, maintaining a robust FE of >90% even at maximum throughput.

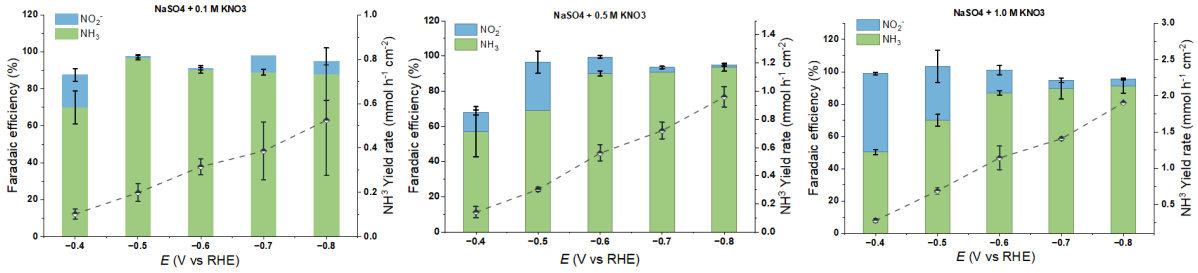


Figure 1 Electrochemical performance of unsupported Co-NC powder across increasing KNO_3 concentrations (0.1 M, 0.5 M, and 1.0 M from left to right). Faradaic efficiency (bars, left axis) and NH_3 yield rate (line, right axis) vs. applied potential.

4.2 The 3D Support Trap and Morphological Analysis

Integrating the Co-NC catalyst onto a 3D porous iron (Fe) foam was hypothesized to boost mass transport and increase the electrochemically active surface area. Scanning Electron Microscopy (SEM) confirmed successful in-situ growth, decorating the macroporous Fe struts with dense catalyst agglomerates (Figure 2, right), compared to the open nanosphere network of the unsupported powder (Figure 2, left).

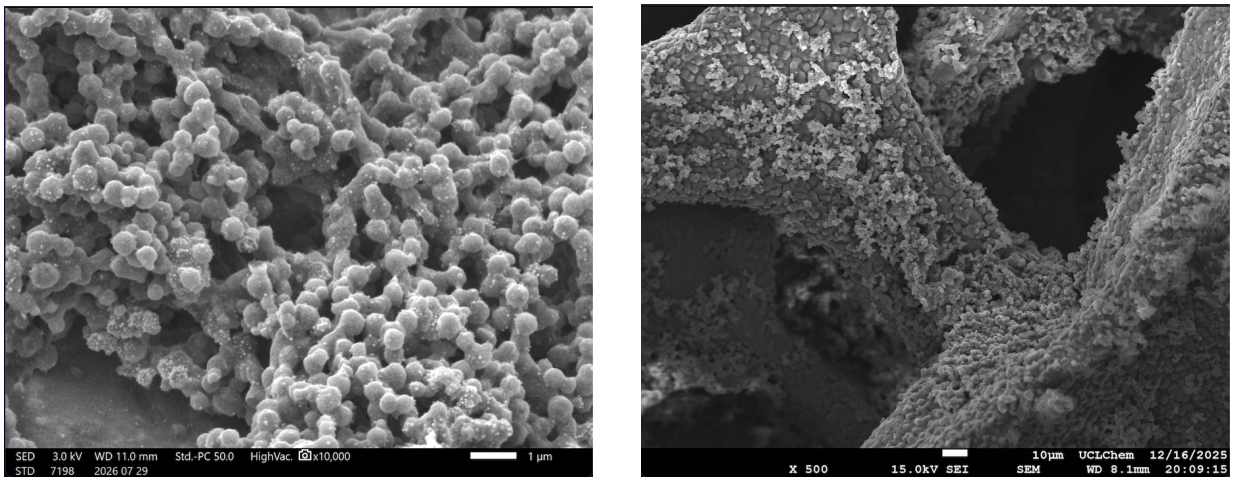


Figure 2 SEM morphological comparison between the open Co-NC nanosphere network (left) and the macroscopic voids and coated struts of the Co-NC@Fe foam (right).

However, electrochemical testing revealed a severe performance collapse for the supported

architecture (Figure 3). The absolute yield rate crashed to <0.4 mmol h^{-1} cm^{-2}, and the peak FE dropped to ~88%. As discussed in the subsequent section, this collapse is attributed to parasitic hydrogen evolution and macroscopic gas trapping within the foam structure.

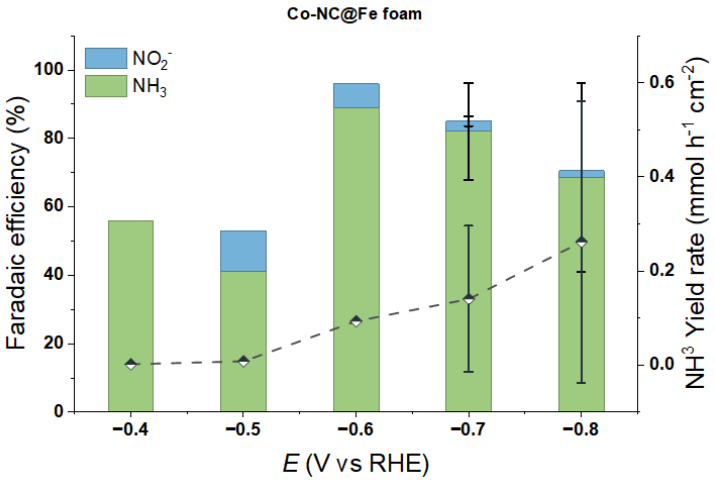


Figure 3 Electrochemical performance of the Co-NC@Fe foam architecture in 0.1 M KNO_3, showing significantly reduced yield and FE.

5 Discussion

The stark contrast in performance between the unsupported Co-NC powder and the Co-NC@Fe foam highlights a critical architectural lesson in electrocatalyst scale-up. The failure of the 3D support stems from the intrinsic electrochemistry of the iron framework, which is highly active for water splitting.

Under applied reductive potentials, the exposed Fe foam acted as a parasitic sink, hijacking electrons to generate hydrogen (H_2) gas instead of reducing nitrate. Furthermore, the deep macroscopic voids of the 3D foam effectively trapped these evolved gas bubbles, physically blocking the liquid electrolyte from reaching the active sites. This phenomenon, which we term the "Support Trap," actively suffocates the ammonia yield.

In contrast, the unsupported Co-NC powder forms an open, interconnected nanosphere network. This morphology avoids the creation of dead zones, maintains constant liquid electrolyte contact, and facilitates rapid gas-product desorption, validating it as the significantly superior catalytic architecture for high-throughput NO_3^-RR.

6 Limitations and Future Work

- **Product balance is incomplete.** Only NH_3 and NO_2^- were quantified; the combined FE in several conditions (e.g., 0.1 M KNO_3 at −0.5 and −0.7 V, both ≈98%) is close to but not exactly 100%, and HER, N_2/N_2O, and NH_2OH were not directly measured. *Next step:* quantify H_2 by gas chromatography and screen for $N_2/N_2O/NH_2OH$ by GC or colorimetric assays, as done for several catalysts in Table 1, to close the electron/nitrogen mass balance.
- **No isotope-labeling control.** The NH_3 measured is assumed to originate from the added $^{14}NO_3^-$, but this study does not include a $^{15}NO_3^-$-labeled control or an open-circuit/no-nitrate blank, both of which are standard controls in the reviewed literature to rule out ambient

nitrogen contamination [1, 6, 7]. *Next step:* repeat the highest-performing condition with $^{15}NO_3^-$ and ^{1}H-NMR quantification.

- **No long-term stability data.** All results reported here are from single potentiostatic runs; multi-cycle or extended (multi-hour to multi-day) stability tests, which are standard in the reviewed literature (e.g., 24–111 h continuous operation [7, 8]), are not included. *Next step:* run consecutive-cycle and long-duration chronoamperometry with post-test structural characterization (SEM/TEM/XRD) to confirm Co-NC retains its structure and performance.
- **Large error bars at some conditions.** Several points (e.g., 1.0 M KNO_3 at −0.5 V, or Co-NC control at −0.5 V) show substantial run-to-run variability. *Next step:* increase the number of replicate measurements at these conditions and report standard deviations explicitly rather than reading approximate ranges from bar-chart error bars.
- **Single-cell configuration.** All data are from an H-cell, which is mass-transport-limited relative to flow cells or membrane-electrode assemblies used to demonstrate industrially relevant current densities in the literature (e.g., >1 A cm^{-2}) [1, 7]. *Next step:* evaluate Co-NC in a flow-cell or MEA configuration to assess performance at higher current density.

7 Conclusion and Future Outlook

The MOF-derived Co-NC powder is a highly selective catalyst (~96% FE) that achieves a commercial-scale NH_3 yield of ~1.9 mmol h^{-1} cm^{-2} when scaled to 1.0 M KNO_3 to overcome diffusion limits. Conversely, the 3D Co-NC@Fe foam suffered a severe performance crash. The foam's intrinsic Hydrogen Evolution Reaction (HER) activity and deep macroscopic pores trapped H_2 bubbles, physically suffocating the NO_3^-RR pathway.

This proves the unsupported, open nanosphere morphology is significantly superior. Future reactor designs must prioritize non-trapping architectures to prevent gas buildup and maximize liquid electrolyte contact for decentralized green ammonia synthesis.

References

[1] Shuhe Han et al. "Ultralow overpotential nitrate reduction to ammonia via a three-step relay mechanism". In: *Nature Catalysis* 6 (2023), pp. 402–414. DOI: 10.1038/s41929-023-00951-2.

[2] Phebe H. van Langevelde, Ioannis Katsounaros, and Marc T. M. Koper. "Electrocatalytic Nitrate Reduction for Sustainable Ammonia Production". In: *Joule* 5 (2021), pp. 290–294. DOI: 10.1016/j.joule.2020.12.025.

[3] M. Duca and M. T. M. Koper. "Powering denitrification: the perspectives of electrocatalytic nitrate reduction". In: *Energy & Environmental Science* 5 (2012), pp. 9726–9742.

[4] Yunpeng Zuo et al. "Capturing Copper Single Atom in Proton Donor Stimulated O-End Nitrate Reduction". In: *Advanced Materials* 37 (2025), p. 2415632. DOI: 10.1002/adma.202415632.

[5] Qinyue Wu et al. "Insights into lattice oxygen and strains of oxide-derived copper for ammonia electrosynthesis from nitrate". In: *Nature Communications* 16 (2025), p. 3479. DOI: 10.1038/s41467-025-58811-5.

[6] Huimin Liu et al. "Efficient Electrochemical Nitrate Reduction to Ammonia with Copper-Supported Rhodium Cluster and Single-Atom Catalysts". In: *Angewandte Chemie International Edition* 61 (2022), e202202556. DOI: 10.1002/anie.202202556.

[7] Yingying Zou et al. "MOF-on-MOF Heterostructured Electrocatalysts for Efficient Nitrate Reduction to Ammonia". In: *Angewandte Chemie International Edition* 63 (2024), e202409799. DOI: 10.1002/anie.202409799.

[8] Shuo Zhang et al. "Fe/Cu diatomic catalysts for electrochemical nitrate reduction to ammonia". In: *Nature Communications* 14 (2023), p. 3634. DOI: 10.1038/s41467-023-39366-9.